Chapter 23 – EXPERIMENTAL INVESTIGATIONS ON THE VFE-2 CONFIGURATION AT TUBITAK-SAGE, TURKEY

by

Suleyman Kurun

23.1 SUMMARY

In this chapter the experimental results of 65° delta wing configuration with sharp and rounded leading edges carried out at TUBITAK-SAGE Ankara Wind Tunnel in the Second International Vortex Flow Experiment (VFE-2) are presented. Test results include force measurements with six component internal balance and oil flow visualisation.

23.2 NOMENCLATURE

a	=	Speed of sound
$\bar{c}$	=	Mean aerodynamic chord, $= 2c_r / 3$
m	=	Meter
M	=	Mach number, $\equiv V / a$
R_{mac}	=	Reynolds number, $\equiv V_\infty \bar{c} / \nu_\infty$
s	=	Second
C_A	=	Axial Force Coefficient; $= A/q_\infty S$
C_D	=	Drag Force Coefficient; $= D/q_\infty S$
C_L	=	Lift Force Coefficient; $= L/q_\infty S$
LE	=	Leading Edge
V	=	Velocity (with x, y, z components of u, v, w)
α	=	Angle of attack, deg
μ	=	Viscosity
ν	=	Kinematic viscosity, $\equiv \mu / \rho$
ρ	=	Density
q	=	Dynamic pressure, $\equiv \rho V^2 / 2$
∞	=	Freestream conditions

23.3 INTRODUCTION

Experimental and Numerical Solutions have been carried out in NATO Research and Technology Organization (RTO) Applied Vehicle Technology 113 (AVT) Task Group named "Understanding and Modeling Vortical Flows to Improve the Technology Readiness Level for Military Aircraft" between 2003 and 2007. The task

group acted in two facets as CAWAPI and VFE-2. Both numerical and experimental solutions have been carried out in the Second International Vortex Flow Experiment (VFE-2) facet. TUBITAK-SAGE Ankara Wind Tunnel had the participation to the experimental part of the VFE-2 facet. In the vortex-flow research program, the NASA 65° delta wing configuration with sharp and rounded leading edges with different leading edge radius was chosen for new tests concerning additional drag and flow field data. The new experiments were aimed at an extension of the knowledge on the vortical flow around the configuration with sharp and rounded leading edges. The measurements were accompanied by numerical investigations to support the interpretation of the flow physics, and in the present paper only limited experimental details are used. The history of VFE-2 has been described by D. Hummel [23-8] and the authors of the experimental contributions to VFE-2 have presented their work in five separate papers from [23-9] to [23-13]. TUBITAK-SAGE and ONERA presented the work in a collective paper [23-11].

Before VFE-2 work started, experimental results from the National Transonic Facility (NTF) at NASA Langley Research Center on a 65° swept delta wing were already available [23-1]. For one sharp and three rounded leading edges normal force and pitching moment as well as pressure distribution measurements had been carried out for a large variety of Mach numbers and Reynolds numbers. The extensive pressure instrumentation used for experiments at NASA Langley prevented the use of an internal balance. Sting-gauging technique was employed to obtain normal force and pitching moment. Because NASA model was not appropriate for internal balance usage, ONERA models with model numbers 4 and 5 were used in Ankara Wind Tunnel tests. In the wind tunnel experiments at TUBITAK-SAGE, a combination of force measurement and flow visualization were used to characterize the flow behaviour.

23.4 EXPERIMENTAL SET UP AND WIND TUNNEL TESTING

23.4.1 Wind Tunnel

TUBITAK-SAGE Ankara Wind Tunnel (AWT) is a closed circuit horizontal type low subsonic wind tunnel having 10ft x 8ft x 20ft (width x height x length respectively) closed atmospheric test section. Maximum test speed is 90 m/s. Its sketch is given in Figure 23-1.

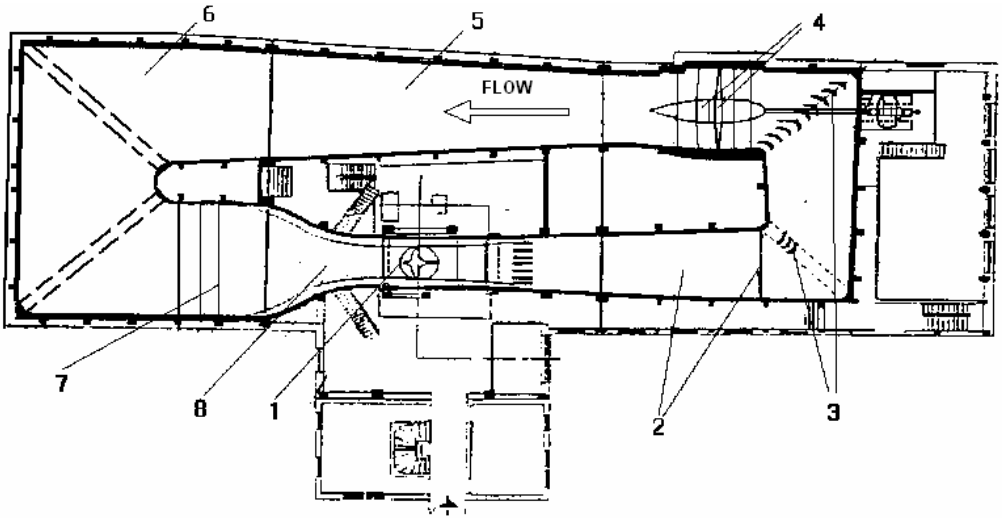

Figure 23-1: Ankara Wind Tunnel Sketch.

23.4.2 Wind Tunnel Model

In the task group 5 models with different sizes and properties according to different test needs were used at different wind tunnels. The model used at National Transonic Facility (NTF) before the task group was called as Model Nr. 0. The list of the models with sizes, owners and tested wind tunnels are given in Table 23-1.

Table 23-1: Wind Tunnel Models Used in VFE-2. [Notations for Leading Edge Shapes: (S) Sharp Edged, (RS) Rounded – Small Radius, (RM) Rounded – Medium Radius, (RL) Rounded – Large Radius]

Model Nr.	Span [m]	Root Chord [m]	Leading Edge	Tested At	Owner
0	0.610	0.653	S, RS, RM, RL	NASA, NTF	NASA Langley RC
1	0.457	0.490	S, RS, RM, RL	NASA, LTPT DLR, TWG ONERA	NASA Langley RC
2	0.933	0.980	S, RM	TU Munich DLR, KKK	TU Munich
3	0.987	1.059	S, RM	Uni. Glasgow	Uni. Glasgow
4	0.457	0.490	S	ONERA TUBITAK-SAGE	ONERA Lille
5	0.457	0.490	RM	ONERA TUBITAK-SAGE	ONERA Lille

ONERA models with model numbers 4 and 5 were used in Ankara Wind Tunnel tests. Two resin one-piece copies of the 'sharp' and 'medium' NASA models were manufactured by ONERA and shipped to Ankara Wind Tunnel. The VFE-2 model is a 65° delta wing with flat upper and lower surfaces. ONERA models tested in Ankara Wind Tunnel has the dimensions equal to NASA model and they are 65° swept symmetrical flat plate delta wings having a root chord length of 0.49023 m, giving a wing area of 0.11207 m^2. The model view is given in Figure 23-2.

Figure 23-2: Wind Tunnel Model.

Shapes were measured along three chord stations situated at Δx = 98.23 mm, 196.23 mm and 392.23 mm from the apex. Results have been compared to the analytical functions and are reported on Table 23-2. It can be observed that discrepancies are of same order when comparing NASA and ONERA 'medium' models with the theoretical shapes. But ONERA 'sharp' variations are twice NASA 'sharp' ones. These differences can be attributed to the fact that ONERA models are made out of resin. Their amplitudes however remain bounded within acceptable limits.

Table 23-2: Geometrical Discrepancy along Three Chord Sections between Each Model and the Analytical Shape: Maximum Variations in mm

Chord Section		NASA Sharp	NASA Medium	ONERA Sharp	ONERA Medium
x = 98.23 mm	Δz max(+)	0.147	0.162	0.278	0.245
	Δz min(-)	0.147	0.123	0.234	0.235
x = 196.23 mm	Δz max(+)	0.181	0.234	0.278	0.143
	Δz min(-)	0.204	0.157	0.22	0.125
x = 392.23 mm	Δz max(+)	0.112	0.206	0.217	0.216
	Δz min(-)	0.096	0.186	0.181	0.142

Although the models had pressure ports for ONERA's needs, no surface pressure measurement has been done in AWT, only pressure measurements for base drag correction was taken and used.

23.4.3 Test Set-up

Considering the expected forces, it was decided to use the 35 mm sting type six component internal balance having 1000 N normal force, 375 N axial force and 150 N.m pitch moment maximum limits. Before tests some interface modifications of the internal balance with the model and sting have been done. Because the size and shape of AWT's balance was different than ONERA's, a new intermediate part was manufactured. The diameters of the AWT's sting and balance were different than ONERA's, and then a new aft body was manufactured with the same outer shape. Carbon fibre fairing of the sting and wing interface was manufactured according to the analytic descriptions provided by NASA and ONERA to be sure that the entire model/sting geometry replicated the original test. The six component internal balance was located between the model and the sting and was used measure the steady and unsteady forces acting on the wing. This balance is cylindrical and care was taken to ensure that there was no transmission of loads from the fairings. An inclinometer was used to measure model angle of attack to within 0.05°. These interfaces are shown on Figure 23-3.

Figure 23-3: Model-Internal Balance-Sting Interface.

Because existing Model Support System was designed for missile testing with less normal force, it couldn't overcome the high normal forces; therefore it became necessary to change the motor. Although new model support system has the capability to fix the model in the tunnel center, the existing system in test dates didn't have this capability. The test set-up views are given in Figure 23-4 and Figure 23-5.

Figure 23-4: Test Set-up 1.

Figure 23-5: Test Set-up 2.

23.4.4 Wind Tunnel Testing

The experiments were carried out in the 3.05 x 2.44 meter, closed circuit, Ankara Wind Tunnel of TUBITAK-SAGE. Tests were conducted at Reynolds numbers of 1.5 million based on the 326.82 mm mean aerodynamic chord. Tests have been done in two phases. In the first phase, force measurements have been done with two models from -4° to +30° with 1° increment. Force and moment data were recorded for the models at each angle of attack. In the second phase, china clay and oil flow visualization studies were conducted.

Investigations on the laminar/turbulent transition on delta wings had been tried to be made. China Clay method is based on shear stress variation. The china clay method of boundary layer flow visualization is a technique for discerning the area of transition from laminar to turbulent flow. The technique is based on the different evaporative qualities of flow in laminar, turbulent and transition regions. China clay, also known as Kaolin, is a ceramic raw material and also used in paper production and in many different industrial applications. A mixture of Kaolin and Kerosene is applied to the model immediately before testing equally and thinly. When the wind is turned on it causes the kerosene to evaporate, leaving streaks of clay powder in the form of the flow pattern. The fluid is dried earlier in a turbulent boundary layer region than a laminar boundary layer region and then, the transparent liquid changes back into white color of the powder in the turbulent boundary layer region. Transition point can be determined as the boundary between the dry region in turbulent region and wet region in laminar region on the surface of the model. Several attempts were made at assessing the transition characteristics of the delta wing but the experiments couldn't be readily implemented and didn't give sufficiently good resolution, because wind tunnel main drive characteristics had a negative effect in reaching the test velocities. The time needed to reach the test velocities was around 8 minutes (excluding the pre-operation time) which was too long to catch the flow phenomena sufficiently good. The china clay method was shelved and flow visualization by oil was made.

Oil flow visualization was carried out from 13° to 26° using different steps. A mixture of oil and pigment material was applied to the surface of the delta wing. After the preparation finished, the wind tunnel was

turned on and reached to test speeds. The flow pattern developed on the surface of the model and then the pictures and films were taken using ultraviolet light and cameras.

23.5 RESULTS

It should be noted that the results presented in the following sections have been corrected for wind tunnel wall interference effects and base drag effects. Although the balance is six component type balances, because of model symmetry only normal force, axial force and pitching moments have been taken into consideration.

23.5.1 Oil Flow Visualization Results

Oil flow visualizations with both models have been made. Only half portions of the models have been used in these tests. Flow visualization pictures are given in Figure 23-6 and Figure 23-7 for sharp and medium radius leading edges respectively.

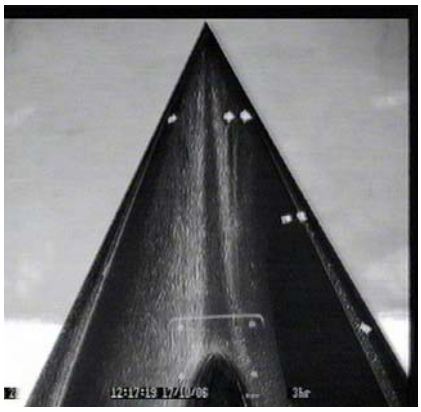 13°	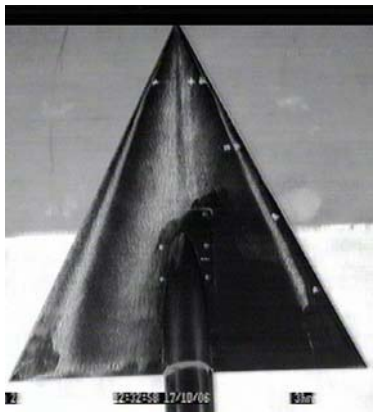 16°
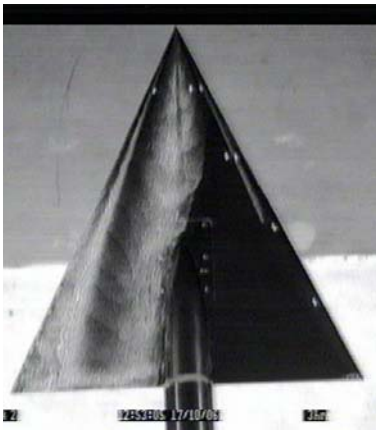 19°	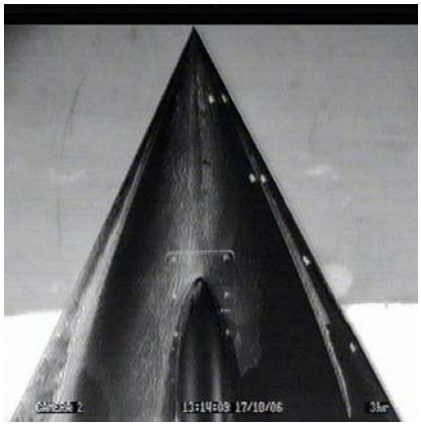 21°
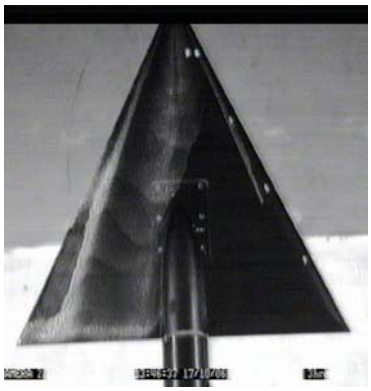 23°	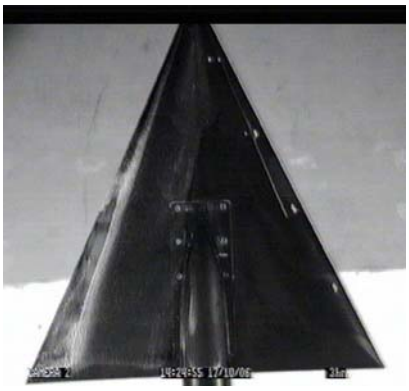 26°

Figure 23-6: Sharp LE Oil Flow Visualization Pictures.

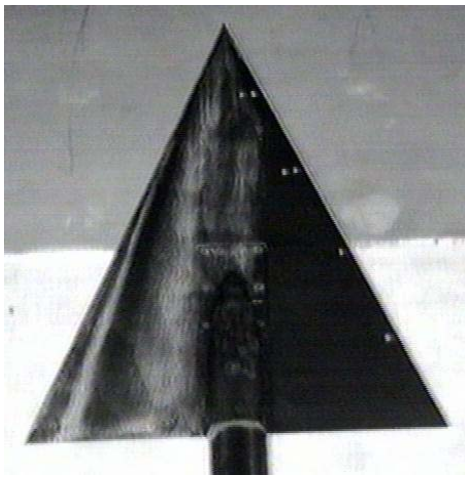 13°	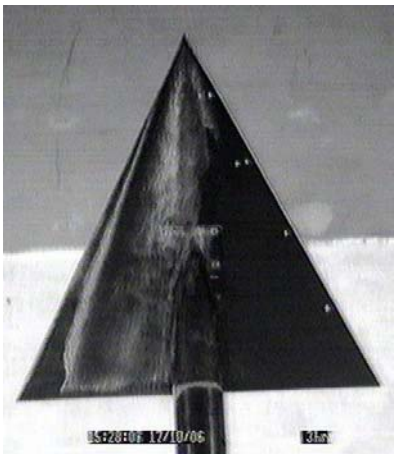 16°
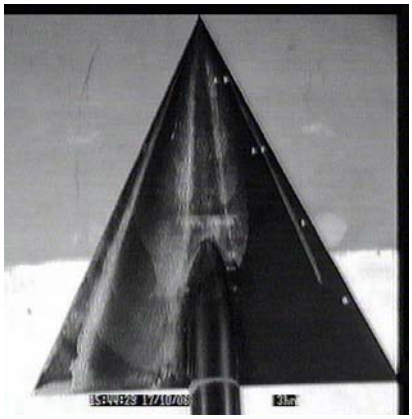 19°	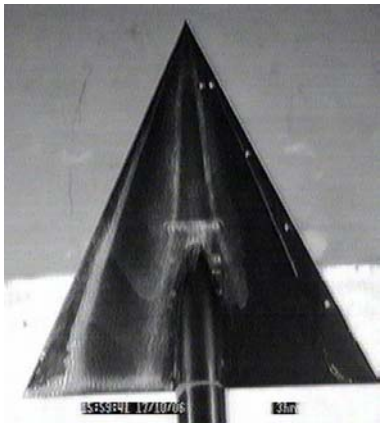 21°
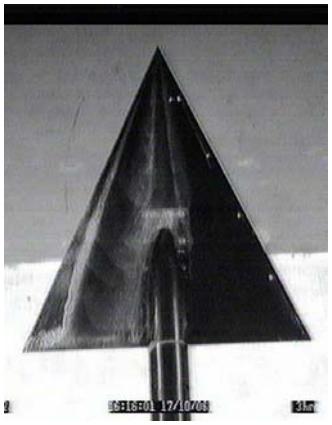 23°	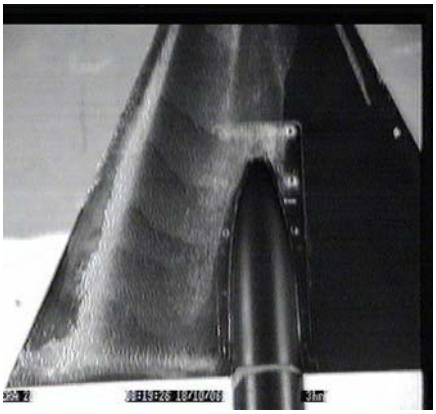 25°

Figure 23-7: Medium Radius LE Oil Flow Visualization Pictures.

Sharp leading edge pictures show expected classical delta wing leading edge vortex system. Flow separation takes place at the leading edge and this separation creates the vortex system above the wing. It can be seen that the vortex system starts from the apex of the wing and goes to the trailing edge. Secondary separation line in many images makes clear the primary and secondary vortex core locations. It can't be observed clearly from the images that there is a vortex breakdown for the angle of attacks higher than 23° but there is evidence of a loss in coherence of the flow structures near the trailing edge. This behaviour may be caused by the progression of vortex breakdown. The first obvious difference between sharp LE and medium LE result is that the primary vortex structure on the rounded edged wing doesn't begin from the apex. Instead, it appears to have its origins at about 10 – 15% of the root chord down the leading edge. An additional structure on the inboard sections is sensed and this structure appears to start near the apex and may be the inboard vortex suggested by the committee. Flow field data is necessary to be sure about the vortex structure. Oil flow visualizations show the same behaviour with the other companies' tests in the task group. Flow visualization results have been compared with oil flow visualization results of the Munich TU and Glasgow University, PSP measurements of DLR and also many computational results and it is seen that there is a good agreement.

23.5.2 Force-Moment Measurement Results

In this section force-moment measurements are going to be given. Normal force, axial force and pitching moments have been taken into consideration and the results are also compared with ONERA results.

Force measurement results are given in Figure 23-8. Normal force and pitch moment results are not very different for two leading edges however the axial force coefficient starts to differ after 6° angle of attack. This may be caused by the flow phenomena described before.

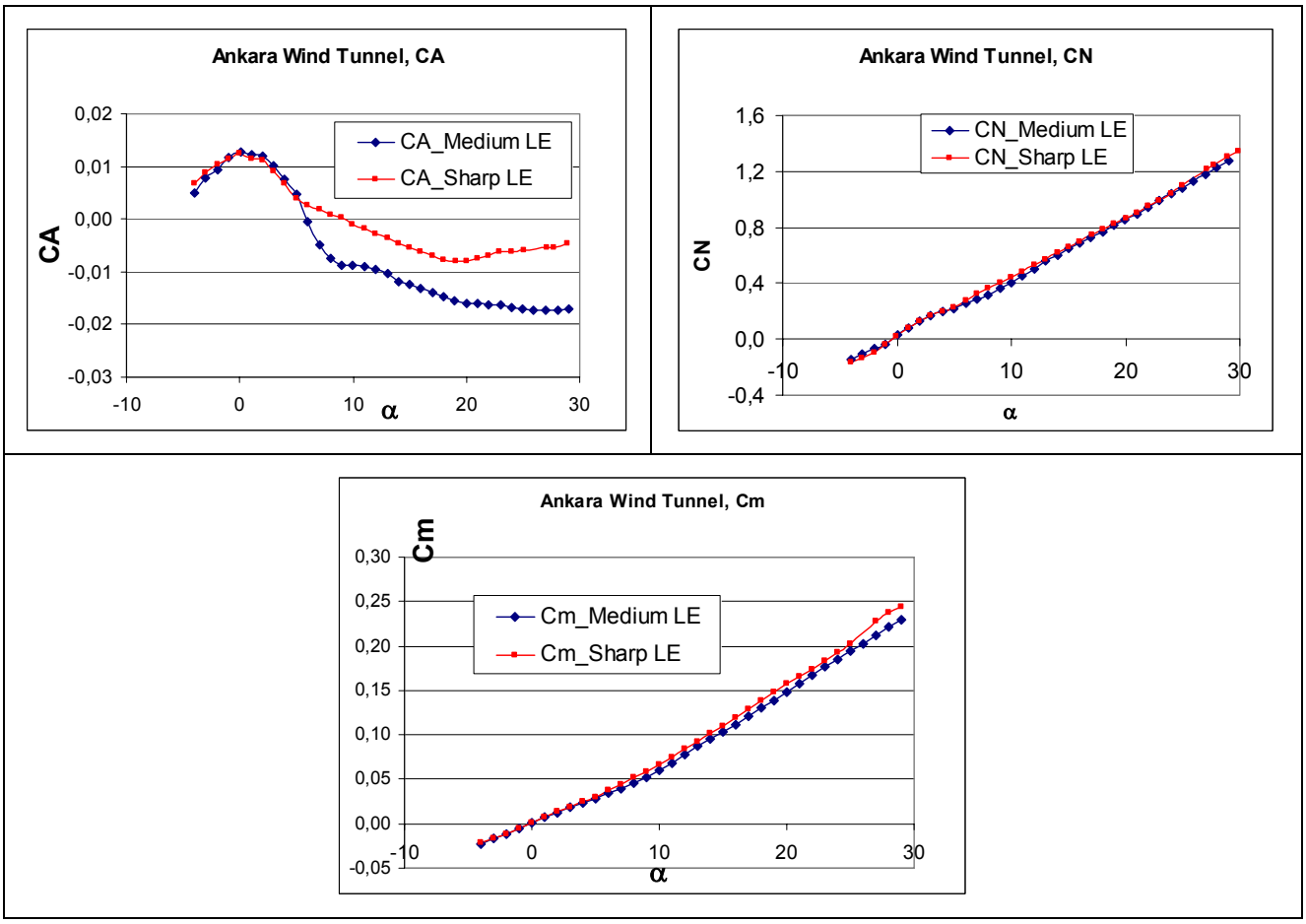

Figure 23-8: Ankara Wind Tunnel Force-Moment Results.

Comparisons have been made with the ONERA results in the following figures. Note that tests have been undertaken in two different wind tunnels at ONERA with open and closed test sections. Although the models are the same, the effects of different wind tunnels with different model support system, internal balance, data acquisition and other items can affect the results. It also has to be considered that ONERA tests were done 1 million Re number instead of 1.5 million.

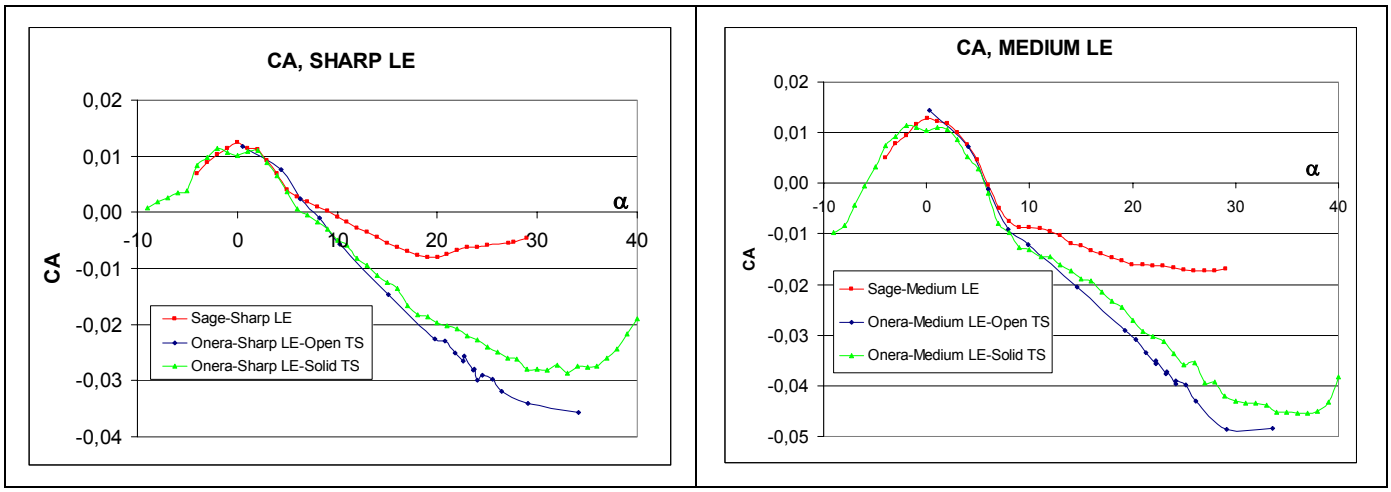

Figure 23-9: Axial Force Comparison.

As the angle of attack increases, the differences in the results increase for both type leading edges. Although it is not shown here, similar comparison has been made with University of Glasgow results and it was seen that the results don't coincide well.

As seen from the Figure 23-10, normal force results show a good agreement. The comparison with University of Glasgow results is also quite well.

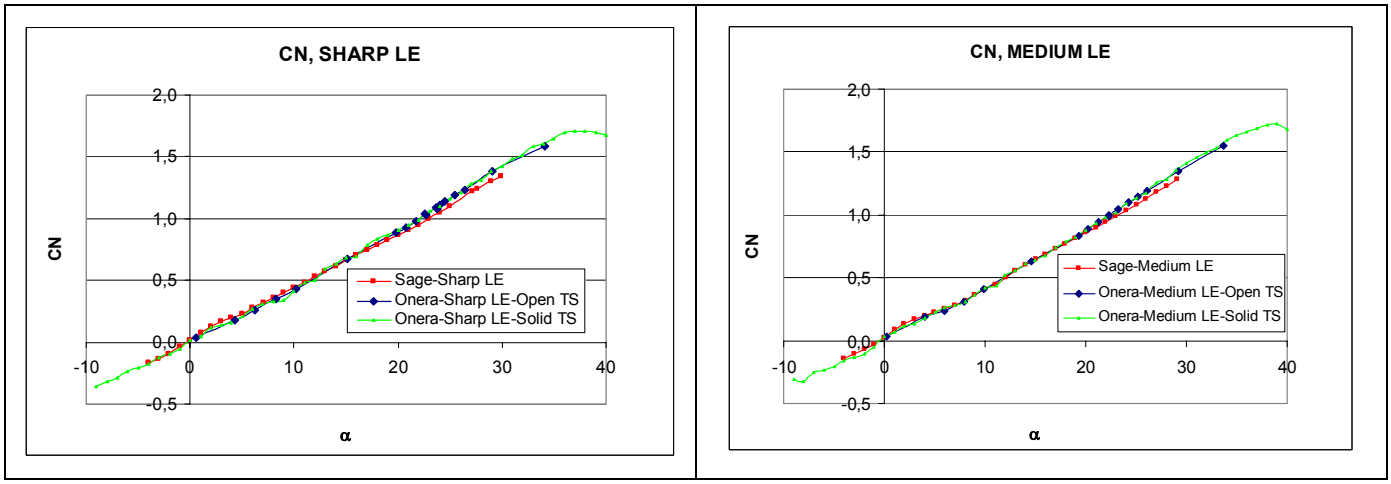

Figure 23-10: Normal Force Comparison.

As seen from the Figure 23-11, pitching moment results show a good agreement. The comparison with University of Glasgow results is also quite well.

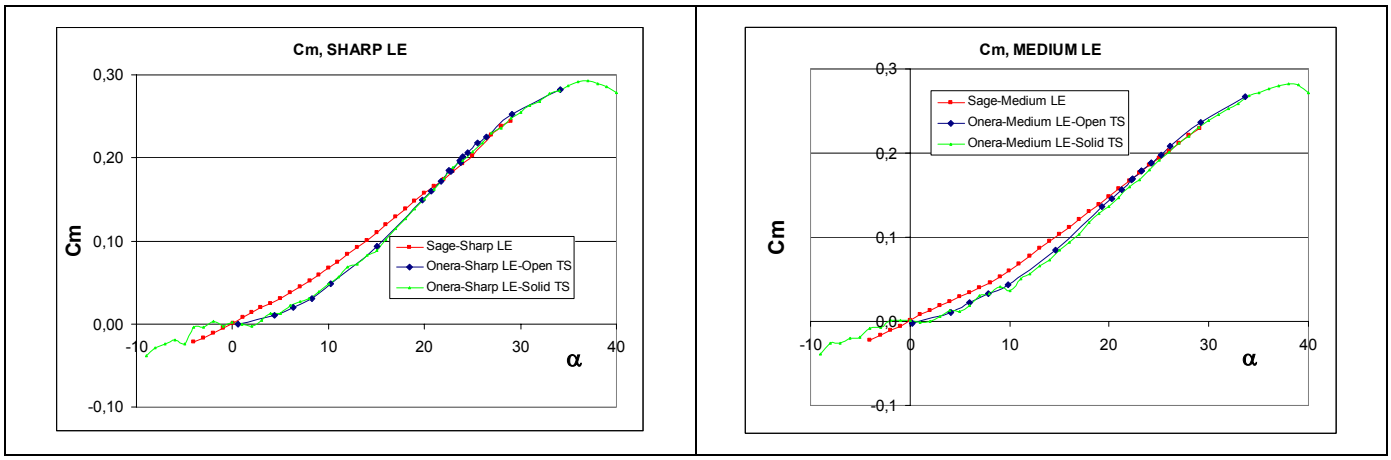

Figure 23-11: Pitching Moment Comparison.

As seen from the Figure 23-12 and Figure 23-13, drag force and lift force results show very good agreement.

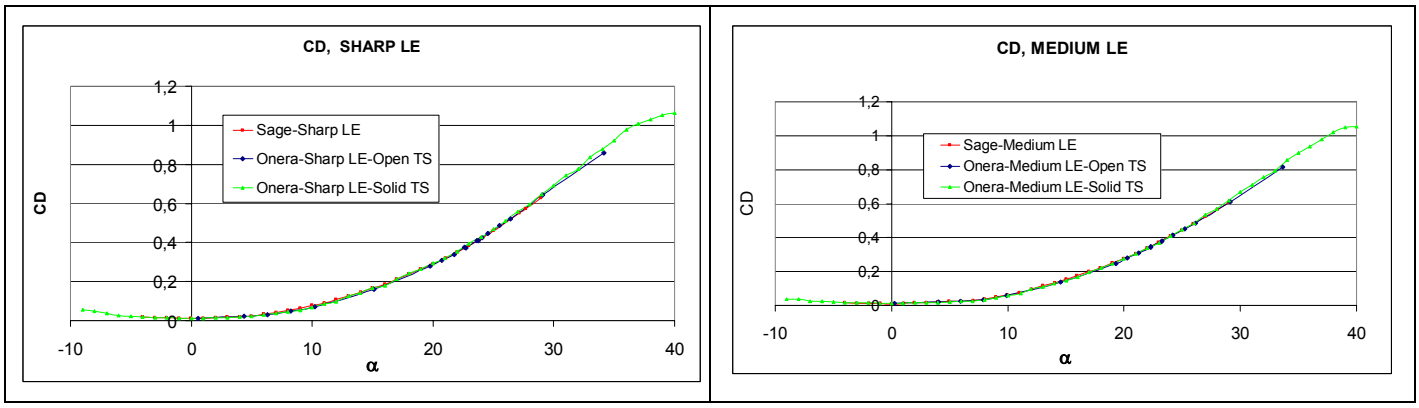

Figure 23-12: Drag Force Comparison.

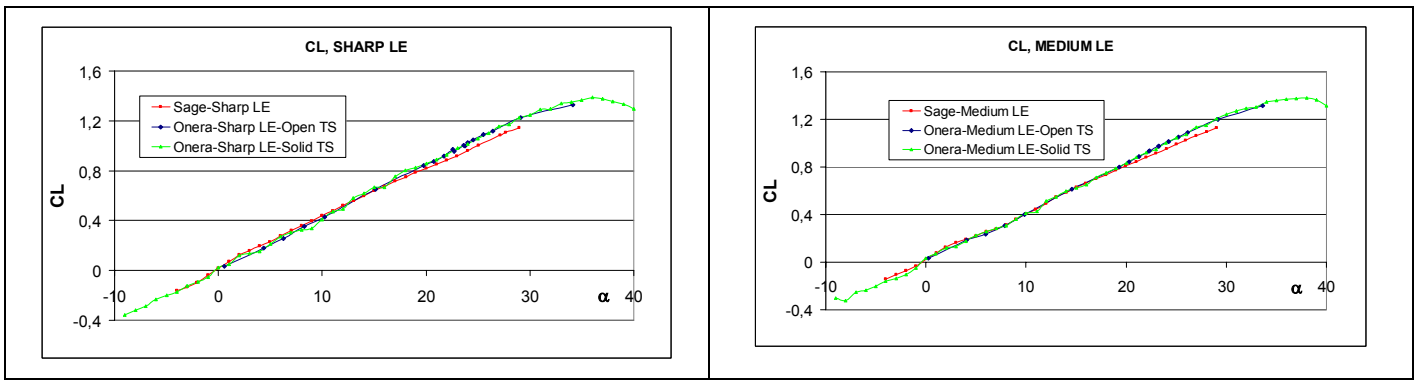

Figure 23-13: Lift Force Comparison.

Force and moment data for Sharp LE and Medium LE is given in Table 23-3 and Table 23-4 respectively.

Table 23-3: Force-Moment Data for Sharp LE

α	CA	CN	Cm	CD	CL
-4.00	4.0000	-0.1644	-0.0220	-0.1644	-0.0220
-3.01	3.0100	-0.1343	-0.0169	-0.1343	-0.0169
-2.01	2.0100	-0.0988	-0.0112	-0.0988	-0.0112
-0.99	0.9915	-0.0374	-0.0046	-0.0374	-0.0046
-0.01	0.0129	0.0176	0.0010	0.0176	0.0010
1.02	-1.0200	0.0760	0.0075	0.0760	0.0025
2.02	-2.0200	0.1288	0.0134	0.1288	0.0084
2.98	-2.9800	0.1660	0.0193	0.1660	0.0143
3.98	-3.9800	0.1954	0.0246	0.1954	0.0246
4.98	-4.9800	0.2298	0.0305	0.2298	0.0305
5.99	-5.9900	0.2772	0.0372	0.2772	0.0372
7.02	-7.0200	0.3229	0.0444	0.3229	0.0444
8.00	-8.0000	0.3631	0.0518	0.3631	0.0518
9.02	-9.0200	0.4041	0.0593	0.4041	0.0593
9.99	-9.9900	0.4459	0.0674	0.4459	0.0674
10.99	-10.9900	0.4846	0.0747	0.4846	0.0747
12.00	-12.0000	0.5316	0.0840	0.5316	0.0840
13.01	-13.0100	0.5714	0.0920	0.5714	0.0920
14.02	-14.0200	0.6166	0.1012	0.6166	0.1012
15.01	-15.0100	0.6591	0.1103	0.6591	0.1103
16.00	-16.0000	0.7009	0.1193	0.7009	0.1193
17.01	-17.0100	0.7452	0.1290	0.7452	0.1290
18.04	-18.0400	0.7866	0.1382	0.7866	0.1382
19.01	-19.0100	0.8298	0.1475	0.8298	0.1475
20.02	-20.0200	0.8694	0.1570	0.8694	0.1570
21.01	-21.0100	0.9080	0.1657	0.9080	0.1657
22.00	-22.0000	0.9492	0.1745	0.9492	0.1745
22.97	-22.9700	0.9961	0.1834	0.9961	0.1834
24.00	-24.0000	1.0461	0.1927	1.0461	0.1927
25.02	-25.0200	1.1029	0.2031	1.1029	0.2031
27.14	-27.1400	1.2171	0.2275	1.2171	0.2275
27.68	-27.6800	1.2452	0.2379	1.2452	0.2379
28.94	-28.9400	1.3047	0.2439	1.3047	0.2439

Table 23-4: Force-Moment Data for Medium LE

α	CA	CN	Cm	CD	CL
-4.02	0.0051	-0.1426	-0.0222	-0.1426	-0.0222
-3.00	0.0078	-0.1067	-0.0164	-0.1067	-0.0164
-1.97	0.0094	-0.0710	-0.0111	-0.0710	-0.0111
-0.99	0.0116	-0.0355	-0.0056	-0.0355	-0.0056
0.04	0.0128	0.0283	0.0009	0.0283	0.0009
1.04	0.0121	0.0839	0.0077	0.0839	0.0027
1.97	0.0119	0.1306	0.0128	0.1306	0.0078
2.98	0.0101	0.1682	0.0189	0.1682	0.0139
3.97	0.0076	0.1950	0.0240	0.1950	0.0240
4.97	0.0047	0.2216	0.0288	0.2216	0.0288
6.00	-0.0004	0.2565	0.0346	0.2565	0.0346
7.01	-0.0049	0.2828	0.0398	0.2828	0.0398
8.02	-0.0075	0.3139	0.0457	0.3139	0.0457
9.01	-0.0088	0.3624	0.0525	0.3624	0.0525
9.99	-0.0088	0.4088	0.0605	0.4088	0.0605
10.98	-0.0089	0.4485	0.0684	0.4485	0.0684
12.02	-0.0094	0.5026	0.0774	0.5026	0.0774
13.01	-0.0103	0.5578	0.0868	0.5578	0.0868
14.03	-0.0119	0.6028	0.0952	0.6028	0.0952
15.04	-0.0124	0.6484	0.1040	0.6484	0.1040
15.97	-0.0133	0.6856	0.1120	0.6856	0.1120
16.98	-0.0140	0.7288	0.1216	0.7288	0.1216
17.98	-0.0148	0.7688	0.1301	0.7688	0.1301
18.98	-0.0154	0.8113	0.1391	0.8113	0.1391
19.99	-0.0161	0.8560	0.1488	0.8560	0.1488
20.99	-0.0161	0.8980	0.1577	0.8980	0.1577
22.00	-0.0162	0.9425	0.1668	0.9425	0.1668
22.99	-0.0163	0.9893	0.1762	0.9893	0.1762
24.03	-0.0167	1.0387	0.1857	1.0387	0.1857
25.01	-0.0170	1.0846	0.1944	1.0846	0.1944
25.97	-0.0173	1.1306	0.2028	1.1306	0.2028
27.00	-0.0173	1.1821	0.2121	1.1821	0.2121
28.02	-0.0173	1.2322	0.2211	1.2322	0.2211
29.04	-0.0170	1.2798	0.2294	1.2798	0.2294

23.6 CONCLUSIONS

Very important results are found from the experiments and the knowledge on delta wing aerodynamics has increased very much. The effect of leading edge type was investigated. Good agreement with other wind tunnels and computational results has been seen in flow visualization and force measurement results.

23.7 ACKNOWLEDGEMENTS

TUBITAK-SAGE is indebted to ONERA for their readiness to provide the wind tunnel models within the scientific program of the Task Group AVT-113. The author would like to thank Ovide Rodriguez (ONERA) for his support of the model loan agreement and transfer of the model form ONERA to TUBITAK-SAGE. The authors would also like to thank to the wind tunnel test team of Ankara Wind Tunnel. Special thanks go to Prof. Dr. D. Hummel (TU Braunschweig) and Dr. John Lamar (NASA Langley) for the initiation of the Task Group AVT-113.

23.8 REFERENCES

[23-1] Chu, J. and Luckring, J.M.: *Experimental Surface Pressure Data Obtained on 65° Delta Wing Across Reynolds Number and Mach Number Ranges*, NASA TM 4645 (1996).

[23-2] Luckring, J.M.: *Reynolds Number and Leading-Edge Bluntness Effects on a 65° Delta Wing*, 40th AIAA Aerospace Sciences Meeting and Exhibit, Reno, 2002.

[23-3] Luckring, J.M.: *Compressibility and Leading-Edge Bluntness Effects for a 65° Delta-Wing*, AIAA Paper 2004-0765, 2004.

[23-4] Luckring, J.M.: *Reynolds Number, Compressibility, and Leading Edge Bluntness Effects on Delta Wing Aerodynamics*, 24th International Congress of the Aeronautical Sciences, Yokohama, 2004.

[23-5] Hummel, D.: *Effects of Boundary Layer Formation on the Vortical Flow Above Slender Delta Wings*, RTO Specialists' Meeting on "Enhancement of NATO Military Flight Vehicle Performance by Management of Interacting Boundary Layer Transition and Separation", Prague, Czech Republic, 4-7 October 2004, Meeting Proceedings RTO-MP-AVT-111, pp. 30-1 to 30-22, 2004.

[23-6] Konrath, R., Klein, C., Engler, R.H. and Otter, D.: *Analysis of PSP Results Obtained for the VFE-2 65° Delta Wing Configuration at Sub- and Transonic Speed*, AIAA-Paper 2006-0060, 2006.

[23-7] Konrath, R., Schröder, A. and Kompenhans, J.: *Analysis of PIV Results Obtained for the VFE-2 65° Delta Wing Configuration at Sub- and Transonic Speeds*, AIAA-Paper 2006-3003, 2006.

[23-8] Hummel, D.: *Review of the Second International Vortex Flow Experiment (VFE-2)*, AIAA Paper 2008-0377, 2008.

[23-9] Luckring, J.M.: *Initial Experiments and Analysis of Vortex Flow on Blunt Edged Delta Wings*, AIAA Paper 2008-0378, 2008.

[23-10] Konrath, R., Klein, Ch. and Schröder, A.: *PSP and PIV Investigations on the VFE-2 Configuration in Sub- and Transonic Flow*, AIAA Paper 2008-0379, 2008.

[23-11] Le Roy, J.F., Rodriguez, O. and Kurun, S.: *Experimental and CFD Contribution to Delta Wing Vortical Flow Understanding*, AIAA Paper 2008-0380, 2008.

[23-12] Furman, A. and Breitsamter, Ch.: *Turbulent and Unsteady Flow Characteristics of Delta Wing Vortex Systems*, AIAA Paper 2008-0381, 2008.

[23-13] Coton, F., Mat, S. and Galbraith, R.: *Low Speed Wind Tunnel Characterization of the VFE-2 Wing*, AIAA Paper 2008-0382, 2008.

[23-14] Luckring, J.M. and Hummel, D.: *What was Learned from the New VFE-2 Experiments*, AIAA Paper 2008-0383, 2008.

[23-15] Nangia, R.K.: *Semi-Empirical Prediction of Vortex Onset and Progression on 65° Delta Wings*, (RTO-AVT-113, VFE-2 facet), AIAA Paper 2008-0384, 2008.

[23-16] Fritz, W.: *Numerical Simulation of the Peculiar Subsonic Flow-Field about the VFE-2 Delta Wing with Rounded Leading Edge*, AIAA Paper 2008-0393, 2008.

[23-17] Gürdamar, E., Ortakaya, Y., Kaya, S. and Korkem, B.: *Some Factors Influencing the Vortical Flow Structures on Delta Wings*, AIAA Paper 2008-0394, 2008.

[23-18] Schiavetta, L.A., Boelens, O.J., Crippa, S., Cummings, R.M., Fritz, W. and Badcock, K.J.: *Shock Effects on Delta Wing Vortex Breakdown*, AIAA Paper 2008-0395, 2008.

[23-19] Cummings, R.M. and Schütte, A.: *Detached-Eddy Simulation of the Vortical Flowfield about the VFE-2 Delta Wing*, AIAA Paper 2008-0396, 2008.

[23-20] Crippa, S. and Rizzi, A.: *Steady, Subsonic CFD Analysis of the VFE-2 Configuration and Comparison to Wind Tunnel Data*, AIAA Paper 2008-0397, 2008.

[23-21] Schütte, A. and Lüdeke, H.: *Numerical Investigations on the VFE 2 65-degree Rounded Leading Edge Delta Wing using the Unstructured DLR-TAU-Code*, AIAA Paper 2008-0398, 2008.

[23-22] Fritz, W. and Cummings, R.M.: *What was Learned from the Numerical Simulations for the VFE-2*, AIAA Paper 2008-0399, 2008.

[23-23] Settles, G.: *Modern Developments in Flow Visualization*, AIAA Journal, Volume 24, No 8, August 1996, pp. 1313-1323.

[23-24] Ura, H., Yokokawa, Y. and Ito, T.: *Experimental Study of Trailing Edge Noise in Low Speed Wind Tunnel*, AIAA Paper 2007-1038, 2007.

[23-25] Greenblatt, D., Paschal, K.B., Yao, C.-S., Harris, J., Schaeffler, N.W. and Washburn, A.E.: *Experimental Investigation of Separation Control Part 1: Baseline and Steady Suction*, AIAA Journal, Vol. 44, No. 12, December 2006, pp. 2820-2830.